# Multi-objective Robust Optimization and Decision-Making Using Evolutionary Algorithms

Deepanshu Yadav
Indian Institute of Technology Madras
Chennai, Tamil Nadu, India
deepanshu.yadav380@gmail.com

Palaniappan Ramu
Indian Institute of Technology Madras
Chennai, Tamil Nadu, India
palramu@iitm.ac.in

Kalyanmoy Deb
Michigan State University
East Lansing, Michigan, USA
kdeb@egr.msu.edu

**COIN Report Number 2023004**

## ABSTRACT

Evolutionary multi-objective optimization (EMO) algorithms are predominantly used for solving multi- and many-objective optimization problems to arrive at the respective Pareto front. From a practical point of view, it is desirable for a decision-maker (DM) to consider objective vectors that are less sensitive to the small perturbation in design variables and problem parameters. Such insensitive, yet closer to Pareto-optimal solutions, lie on the so-called *robust* front. In real-world applications, such as engineering design and process optimization problems, perturbations in variables come from manufacturing tolerances, uncertainties in material properties, variations in operating conditions, etc. The existing EMO literature on robustness studies emphasized on finding the entire robust front, but hardly considered robustness in both optimization and decision-making tasks. In this paper, we propose and evaluate different algorithmic implementations of three aspects – multi-objective optimization, robustness consideration, and multi-criterion decision-making – together. Based on experimental results on two to eight-objective problems, we discuss the outcomes and advantages of different integration approaches of these three aspects and present the most effective combined approach. The results are interesting and should pave the way to develop more efficient multi-objective robust optimization and decision-making (MORODM) procedures for handling practical problems with uncertainties.

## CCS CONCEPTS

• **Computing methodologies** → **Optimization algorithms**; • **Theory of computation** → **Stochastic control and optimization**.

## KEYWORDS

Evolutionary Algorithms, Pareto Front, Robust Front, Multi-criteria Decision-making, R-NSGA-III


*GECCO '23, July 15–19, 2023, Lisbon, Portugal*

ACM ISBN 979-8-4007-0119-1/23/07…$15.00
https://doi.org/10.1145/3583131.3590420

**ACM Reference Format:**
Deepanshu Yadav, Palaniappan Ramu, and Kalyanmoy Deb. 2023. Multi-objective Robust Optimization and Decision-Making Using Evolutionary Algorithms. In *Genetic and Evolutionary Computation Conference (GECCO '23), July 15–19, 2023, Lisbon, Portugal.* ACM, New York, NY, USA, 9 pages. https://doi.org/10.1145/3583131.3590420

## 1 INTRODUCTION

Many real-world applications consist of multiple and generally conflicting objectives. For solving such problems, evolutionary algorithms (EAs) are being used, extensively. The outcome of an evolutionary multi-objective algorithm (EMO) is a well-distributed and diverse set of non-dominated solutions represented by a set of Pareto-optimal (PO) solutions [12, 31] lying on a Pareto front (PF). Multi-criteria decision-making (MCDM) techniques compute preferred PO solution(s) following decision maker's (DM's) preferences [4, 20]. The existing MCDM techniques are systematically developed to perform the optimization and decision-making task iteratively. Several MCDM techniques apply the concept of utility functions or scalarization functions using the DM's preference to reformulate the original multi-objective optimization (MOO) problem into a single objective optimization problem and arrive at a single solution favoring the DM's criteria. Achievement scalarization function (ASF) [26, 27] and its augmented version (AASF) [20] are used to develop several MCDM techniques, such as the surrogate worth trade-off (SWT) method [14], GUESS method [3], satisficing trade-off method (STOM) [22], and Pareto Race [17, 18].

In addition, there exist population-based evolutionary MCDM techniques that account for DM's preference in EMO algorithms to arrive at the multiple solutions favoring DM's criteria. Evolutionary MCDM techniques allow the DMs to supply preference information in terms of objective weights, constraint bounds, reference points, and reference directions. Reference point and reference direction-based EMOs (R-EMO) such as R-NSGA-II [13], RD-NSGA-II [9], R-NSGA-III [25], and light beam search [10, 16] are the evolutionary MCDM techniques that have been extensively used in the literature. Contrary to the utility function or scalarization function-based MCDM methods in which only one solution is obtained at the end of each iteration of the algorithm, evolutionary MCDM techniques benefit by providing multiple preferred solutions at the end of each iteration allowing the DM to compare these solutions and choose the most preferred one. The capability of evolutionary MCDM techniques in generating multiple preferred solutions, comparing them, and choosing the preferred solution(s) in each iteration brings flexibility to the decision-making tasks.

In a decision-making task, it is desirable for a DM to arrive at an objective vector or solution that has a small or insignificant effect of perturbation in the corresponding decision variable vector. Such solutions lie on the *robust front* (RF), instead of lying on the PF, have the utmost importance in real-world scenarios including but not limited to engineering design and optimization under uncertainties. An earlier study [8] proposed multi-objective robust optimization (MORO) algorithm using NSGA-II [12] that reformulates the original multi-objective optimization problem (MOP) into a robust MOP by including two robustness definitions to obtain an RF. Later, other MORO techniques [32] were proposed for evaluating RF. The recent literature on MORO techniques for robust optimization is discussed in [6, 15, 24, 30]. Along with problem-specific objectives, the robustness index is used as an additional objective in [6] to compute the RF. [24] transforms an uncertain 3-objective problem into a 5-objective deterministic problem to arrive at the robust solution(s). Considering the fact that obtaining RF is computationally expensive and generally, MCDM techniques find one or more preferred robust solutions that satisfy DMs' preferences, the current study proposes four multi-objective robust optimization and decision-making (MORODM) schemes for evaluating preferred robust solutions and applies one of the robustness definitions to a reference point-based EMO – R-NSGA-III – for robust decision making tasks. The novelty of the current paper is to incorporate uncertainty into practical MOO problems that involve MCDM tasks to arrive at preferred solutions. For this purpose, four different MORODM schemes are proposed and their computational effectiveness is discussed.

The rest of the paper is organized as follows. Section 2 discusses the concept of multi-objective robust optimization (MORO). A brief discussion on multi-objective robust optimization and decision-making (MORODM) using R-NSGA-III is presented in Section 3. Next, the results of the proposed MORODM approach to three test problems and two real-world engineering problems are discussed in Section 4, followed by the conclusions drawn in Section 5.

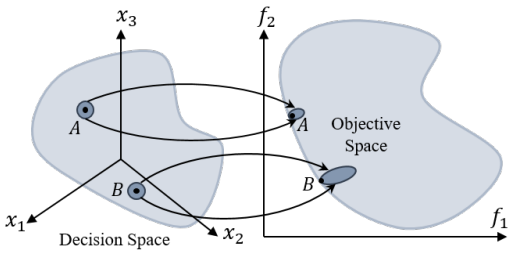


**Figure 1: A and B are two points in decision space. In objective space, solution A is less sensitive as compared to solution B for a small perturbation in design variable space.**

## 2 MULTI-OBJECTIVE ROBUST SOLUTIONS

For the case of multi-objective optimization problems, the concept of robust optimization was introduced and presented in [8]. Consider the following MOO problem:

$$\begin{aligned} \underset{\mathbf{x}}{\text{Minimize}} \quad & \{f_1(\mathbf{x}), f_2(\mathbf{x}), \ldots, f_M(\mathbf{x})\}, \\ \text{subject to} \quad & \mathbf{x} \in \mathcal{S}, \end{aligned} \tag{1}$$

where $\mathcal{S}$ is the feasible variable space. A robust solution $\mathbf{x}$ is defined as the one for which the objective vector $\mathbf{f}(\mathbf{x})$ is insensitive up to a certain level for a perturbation in the neighborhood of $\mathbf{x}$.

Figure 1 illustrates two decision vectors A and B in decision space and their respective response values in objective space. It can be inferred from Figure 1 that a small perturbation in the neighborhood of decision vector B is more sensitive in objective space as compared to decision vector A. Hence, decision vector A is more robust than decision vector B. Also, from a practical point of view, solution A is more important than solution B.

### 2.1 Multi-objective Robust Optimization (MORO) to Find Robust Front (RF)

The following two ideas used in the literature [2] for executing a robust single-objective optimization task, are extended for computing RF in the case of MOO [8]:

(1) **Robust Solution of Type I:** Mean effective objective function is used for optimization instead of the original objective function.
(2) **Robust Solution of Type II:** The normalized difference between the perturbed objective function and the original objective function is used as a constraint to have a better control in defining a robust solution.

The definitions of the Robust Solution of Type I and Type II for multi-objective optimization are presented in [8] as follows:

*Definition 2.1 (**Robust Solution of Type I**).* Defined in a $\delta$-neighborhood $\left(\mathcal{B}_\delta(\mathbf{x})\right)$, a solution $\mathbf{x}^*$ is called a multi-objective robust solution of Type I, if it is a global feasible Pareto-optimal solution to the following multi-objective minimization problem:

$$\begin{aligned} \underset{\mathbf{x}}{\text{Minimize}} \quad & \{f_1^{\text{eff}}(\mathbf{x}), f_2^{\text{eff}}(\mathbf{x}), \ldots, f_M^{\text{eff}}(\mathbf{x})\}, \\ \text{subject to} \quad & \mathbf{x} \in \mathcal{S}, \end{aligned} \tag{2}$$

where $f_j^{\text{eff}}$ is defined as follows:

$$f_j^{\text{eff}} = \frac{1}{\mathcal{B}_\delta(\mathbf{x})} \int_{\mathbf{y} \in \mathcal{B}_\delta(\mathbf{x})} f_j(\mathbf{y}) d\mathbf{y}. \tag{3}$$

In practical applications, the mean effective function $f_j^{\text{eff}}$ expressed in (3) is computed by generating $H$ neighborhood points in the $\mathcal{B}_\delta(\mathbf{x})$ vicinity of a decision vector $\mathbf{x}$ and taking the mean of the objective function $f_j$ at those $H$ neighborhood points. Instead of the original objective functions $f_j$, the mean effective functions $f_j^{\text{eff}}$ are used for optimization. This formulation inherently accounts for the sensitivity of the objective functions due to the small perturbation in decision vector $\mathbf{x}$.

*Definition 2.2 (**Robust Solution of Type II**).* A solution $\mathbf{x}^*$ is called a multi-objective robust solution of Type II, if it is a global feasible Pareto-optimal solution to the following multi-objective

minimization problem:

$$\begin{aligned} \underset{\mathbf{x}}{\text{Minimize}} \quad & \{f_1(\mathbf{x}), f_2(\mathbf{x}), \ldots, f_M(\mathbf{x})\}, \\ \text{subject to} \quad & \frac{||\mathbf{f}^{\text{eff}}(\mathbf{x}) - \mathbf{f}(\mathbf{x})||_2}{||\mathbf{f}(\mathbf{x})||_2} \leq \eta, \\ & \mathbf{x} \in \mathcal{S}, \end{aligned} \tag{4}$$

where $\eta$ is the maximum normalized difference between the original and mean effective objective functions allowed to define a robust solution.

## 2.2 Robust Solution Identification (RSI)

In this paper, for identifying robust solutions from a set of non-dominated (ND) solutions, Type-II definition is applied to pick ND solutions that satisfy the constraint in (4).

# 3 MULTI-OBJECTIVE ROBUST OPTIMIZATION AND DECISION MAKING (MORODM) USING TYPE-II ROBUSTNESS AND R-NSGA-III

Preferred solutions can be found by focusing an EMO algorithm on a part of the PF. Here, we discuss and use the reference-point based EMO (R-EMO) approach. Preferred solutions can also be picked from a set of non-dominated solutions already found by an EMO. We call this task reference-point based multi-objective selection (R-MOS) task.

## 3.1 R-NSGA-III Procedure

In R-NSGA-III, DM provides $K$ reference point(s) in terms of an objective vector that satisfies their aspiration level. After scaling the reference point(s) according to the range of objective functions, the normalized reference points $\bar{r}^{(k)}$ $(k = 1, \ldots, K)$ are obtained as depicted in Figure 2a. Then intercept of the unit hyper-plane in criterion space and vector $\bar{r}^{(k)}$ (obtained on joining the normalized reference point(s) to the ideal point) is computed to arrive at points $\dot{r}^{(k)}$ which lies at unit hyperplane. Next, $r_p = \binom{M+p-1}{p}$ Das-Dennis points $(h_j)$ are created on a unit hyper-plane, using a suitable gap $p$, where $M$ is the number of objective functions [7]. These points are then shrunk using a factor $\mu$ as follows:

$$\bar{h}_j = \mu h_j, \quad \mu \in (0, 1). \tag{5}$$

In the next step, the shrunk Das-Dennis points are projected to the unit hyper-plane along the direction of a vector joining the centroid $(g)$ of shrunk hyperplane and $\dot{r}^{(k)}$, that lie on a unit simplex centered around the projected point $\dot{r}^{(k)}$. These projected points around $\dot{r}^{(k)}$ are the reference points $(r_p)$ for NSGA-III. Upon repeating this procedure for all $K$ supplied aspiration points one by one, $K \times r_p$ reference points are obtained. Adding $M$ extreme points to $K \times r_p$; total $(K \times r_p + M)$ reference points are supplied to the NSGA-III algorithm. In each generation, the points closer to the reference line obtained on joining the reference point with the ideal point $O$, are used for creating offspring. At the end of the NSGA-III run, only the single closest solution for each reference line/direction generated by the original reference points is considered, except the ones corresponding to the extreme reference directions. The DM has to supply the population size per reference point $(r_p)$ and shrinkage factor $(\mu)$ to compute the preferred solutions.

## 3.2 R-MOS Procedure

Given a set of non-dominated (ND) solutions, we can choose the closest $r_p$ solutions to a reference point in the Euclidean sense on the normalized objective space. For multiple, say $K$ reference points, $K \times r_p$ points are equally divided among them.

## 3.3 Four Integration Schemes

Next, we discuss four different MORODM schemes for integrating EMO, reference-point-based multi-objective selection (R-MOS), and robust solution identification (RSI) together for finding respective preferred robust solutions for multi-objective optimization in the following sequences:

**Scheme A:** PF using EMO on original problem → MCDM using R-MOS from PF → RSI on R-MOS solutions using formulation (4).

**Scheme B:** PF using EMO on original problem → RSI from PF using formulation (4) → MCDM using R-MOS from RSI solutions.

**Scheme C:** RF by applying formulation (4) on the original problem (Robust EMO) → MCDM using R-MOS from RF.

**Scheme D:** Robust MCDM solutions by applying formulation (4) in R-EMO (all three concepts are combined together).

Scheme A computes the PF using an EMO algorithm, followed by computing preferred solution(s) using the R-MOS procedure. Finally, the preferred solutions that qualify the robustness definition (4) are marked as the robust solution(s). Scheme B first computes the PF using an EMO algorithm and then discards the solution those do not satisfy the robustness constraint defined in formulation (4) to arrive at an RF. Finally, the R-EMO-based MCDM procedure is used to perform MCDM tasks on the RF. Both of these schemes can only find preferred robust solutions if they lie on the original PF.

Scheme C performs MCDM on the RF, instead of PF, obtained by solving constrained MOO (4) using an EMO algorithm. Then, preferred solutions are picked from the RF using the MCDM approach. Scheme D handles DM's preference information as they are treated in an R-EMO and also uses the robustness definition simultaneously to find preferred robust solutions in a single run and without computing the complete PF or complete RF. Hence, from a computational point of view, Scheme D is expected to be the most efficient among the four schemes, due to the combined parallel efforts of all three concepts in a single algorithm. In the aforementioned schemes, we use NSGA-III as an EMO algorithm and R-NSGA-III as an R-EMO procedure for our proposed MORODM schemes.

# 4 RESULTS

This section presents the results of MORODM schemes discussed in the previous section, applied on three test problems and two real-world engineering examples.

## 4.1 A Bi-objective Test Problem

This test problem has two objectives and five design variables. The details of test problem 1 are discussed in [8]. A well-distributed PF using NSGA-III algorithm is computed and presented in Figure 2b. For this problem, 100 reference directions are created using the Das-Dennis method [7]. Next, NSGA-III is executed for 200

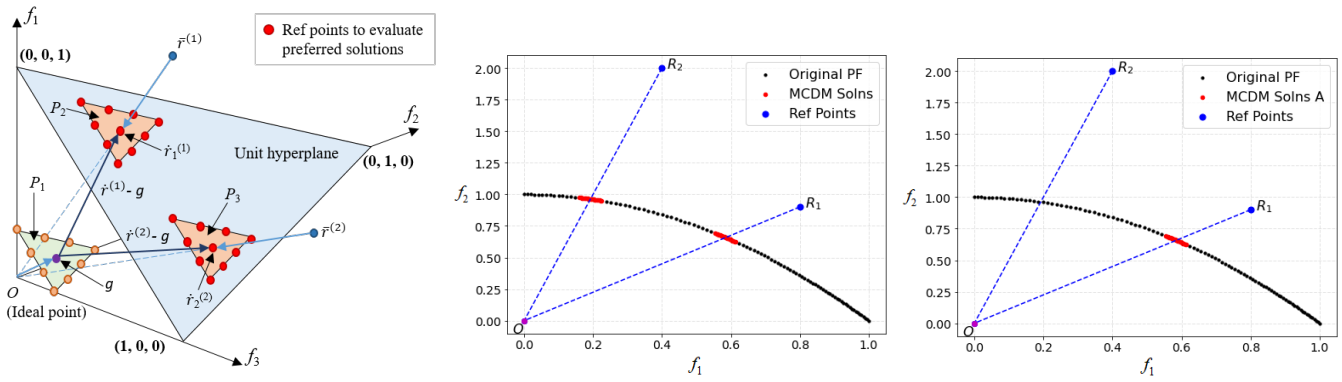


**(a) Reference point based-NSGA-III procedure** **(b) MCDM on PF** **(c) MORODM using Scheme A**

**Figure 2: (a) A sketch of the R-NSGA-III's reference point computation procedure. $\bar{r}^{(1)}$ and $\bar{r}^{(2)}$ are reference points provided by DM. $P_1$ is the shrunk hyperplane depending on the parameter $\mu$. $P_2$ and $P_3$ are reference planes on the unit hyperplane corresponding to the DM preferences $\bar{r}^{(1)}$ and $\bar{r}^{(2)}$. $\dot{r}^{(1)}$ and $\dot{r}^{(2)}$ are the intercept of unit hyperplane and normalized reference point vectors $\bar{r}^{(1)}$ and $\bar{r}^{(2)}$, (b) MCDM on the bi-objective test problem, (c) MORODM on the bi-objective test problem using Scheme A. In the scatter plot, the black markers represent PF obtained using NSGA-III. $R_1$ and $R_2$ are reference points. The red dots represent the MCDM solutions obtained using R-NSGA-III. $O$ is the ideal point.**

generations with a tournament selection strategy in *pymoo* [1]. While implementing NSGA-III, other parameters used are binary crossover ($\eta_c = 30$, $p_c = 1.0$), mutation ($p_m = 1/n$, $\eta_m = 20$).

Consider two reference points $R_1 = [0.8, 0.9]$ and $R_2 = [0.4, 2.0]$ as DM's criteria to evaluate the preferred solutions. We perform MCDM using R-NSGA-III to compute the preferred solutions corresponding to the reference points $R_1$ and $R_2$ presented in red color markers in Figure 2b. With a shrinkage factor value of $\mu = 0.05$ and population size per reference point $r_p = 20$, R-NSGA-III algorithm is executed for 500 generations. It is to be noted that these preferred solutions are PO solutions that need to be checked for Type-II robustness.

The four MORODM schemes discussed in Section 3 for performing robust MCDM tasks are implemented for this problem. In implementing these four MORODM schemes, the robustness parameters, namely, $\delta$, $H$, and $\eta$ are kept constant. Given the design variables ($x_i$), the perturbations used are $\delta_i = 2\delta$ ($i = 2, 3, 4, 5$) and $\delta_1 = \delta$, where $\delta = 0.007$. The number of neighboring points $H$ is set to 100 and the normalized difference in original and effective function $\eta$ is set to 0.4. The strategy for generating the neighboring solutions in the vicinity of a decision variable point is being adopted from [8], where Latin Hypercube Sampling (LHS) was performed. In Scheme A, the MCDM solutions obtained on PF (red markers in Figure 2b) are checked for their robustness using (4). Figure 2c presents PF and reference points $R_1$ and $R_2$, along with the preferred robust solutions in red color marker obtained by implementing the MORODM Scheme A. It is to be noted from Figure 2c that, no robust MCDM solutions are obtained corresponding to the reference point $R_2$. This is due to the fact that the MCDM solutions corresponding to reference point $R_2$ obtained in Figure 2b do not satisfy the Type-II robustness definition. However, MCDM solutions corresponding to reference point $R_1$ qualify the robustness definition (4) and constitute the only MORODM solutions according to Scheme A.

Next, we implement Scheme B for performing the MORODM task. Solutions with green dots are obtained from the PF (black dots) using Type-II robustness definition (4). Next, the preferred solutions from the set of green dots are chosen using the RSI approach used in R-NSGA-II. The preferred robust solutions of Scheme B are marked in red dots in Figure 3a. It can be inferred that no preferred robust solution is found for reference point $R_2$ by Scheme B.

The two MORODM Schemes A and B implemented on bi-objective test problems require the computation of PF followed by performing a robustness check and MCDM task in different orders. Next, we introduce the Scheme C that instead of first computing PF, computes the RF first by solving the MOO defined in (4). Figure 3b represents the RF (in green dots) obtained by solving the Type-II MORO problem (4) using NSGA-III algorithm. Next, the MCDM task is performed on the RF instead of PF. Given two reference points $R_1$ and $R_2$, MCDM task is executed using R-NSGA-III procedure to arrive at robust MCDM solutions highlighted in red dots. The GA parameters used for NSGA-III and R-NSGA-III are kept the same as in Scheme A except for the number of generations in R-NSGA-III is set to 1,000. It is to be noted that some parts of the PF and RF are identical. On smaller $f_1$ values, the PF solutions are sensitive and hence are not robust. A new RF appears there. This shift now allows the DM to evaluate and obtain the robust solutions corresponding to reference point $R_2$ that was not available in the case of MORODM Schemes A and B. However, it comes at the computation cost of performing the MORO task.

Acknowledging the fact that upon performing the MCDM on the RF in MORODM Scheme C, only a few preferred robust solutions are saved and others are discarded, we introduce Scheme D that applies the Type-II robustness definition and performs decision-making

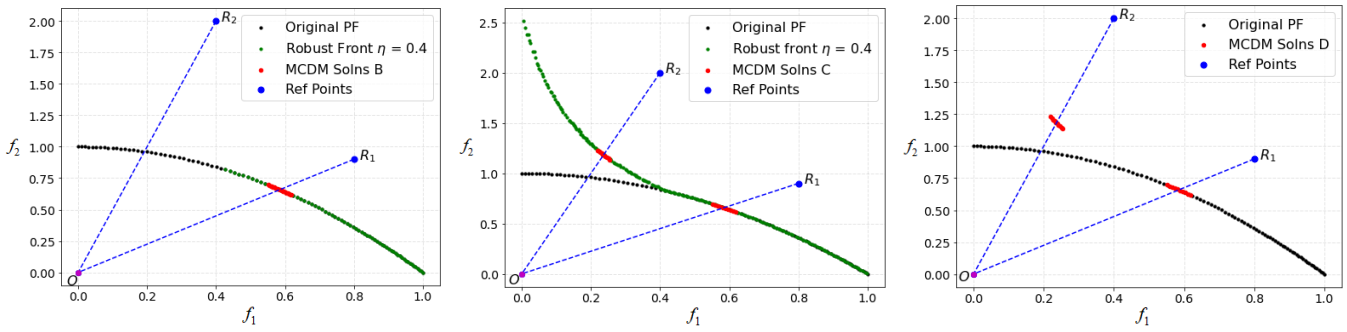


(a) MORODM using Scheme B (b) MORODM using Scheme C (c) MORODM using Scheme D

**Figure 3: Bi-objective test problem: In the scatter plot, the black markers represent PF obtained using NSGA-III. The green dots represent the RF. The red dots represent the preferred robust solutions.**

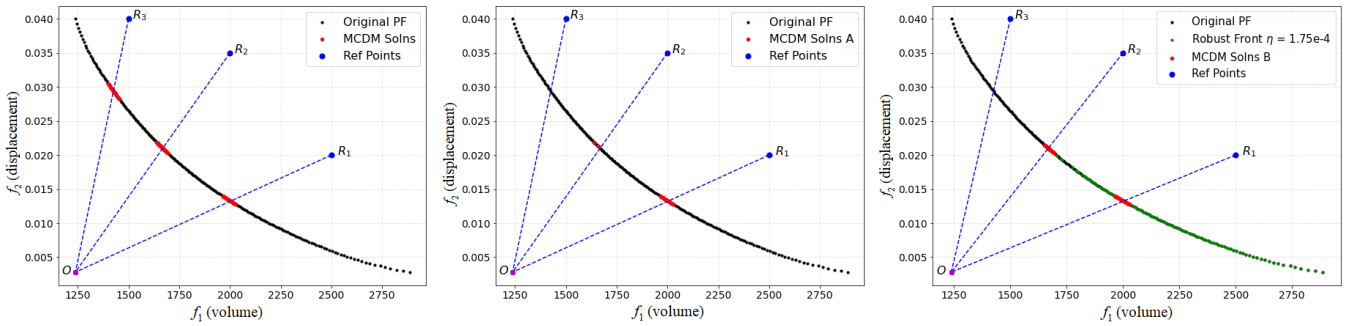


(a) MCDM solutions on PF (b) Robust MCDM using MORODM Scheme A (c) Robust MCDM using MORODM Scheme B

**Figure 4: 4-bar truss problem results are shown. Black dots represent PF obtained using NSGA-III. Green dots represent the obtained RF. The red dots represent the preferred robust solutions.**

simultaneously for MORODM task using R-NSGA-III procedure and computes only preferred robust solution instead of evaluating the complete PF or RF. Scheme D performs the MORODM task that avoids evaluating the complete RF to save the computational cost of MORO and MaORO algorithms. Figure 3c represents the evaluated preferred robust solutions in red dots. Reference points $R_1$ and $R_2$, shrinkage factor $\mu = 0.05$, and the population size per reference point $r_p = 20$ is supplied to R-NSGA-III algorithm to perform MORODM. The GA parameters were kept the same except for the number of generations was set to 2,000. The preferred robust solutions of Scheme D are identical to that obtained in Scheme C. However, it is to be noted that in Scheme D for MORODM neither PF nor RF is computed; this reduces the computational cost of evaluating the PF and RF.

## 4.2 4-Bar Truss Problem (Bi-objective)

The 4-bar truss design problem is an unconstrained bi-objective problem that has four decision variables. The first objective is structural volume and the second objective is joint displacement. Further details on this problem can be found in [5]. For variables $x_i$, the perturbation $\delta_i = 2\delta$ $(i = 1, 2, 4)$ and $\delta_3 = \delta$ is used. $H = 50$ solutions are generated in the neighborhood of a design point $\mathbf{x}$ by setting the parameter $\delta$ and $\eta$ to 0.25 and $1.75 \times 10^{-3}$, respectively, while implementing Type-II robustness definition (4). The four MORODM schemes are applied to the 4-bar truss problem for obtaining preferred robust solutions for three reference points: $R_1 = [2500, 0.02]$, $R_2 = [2000, 0.035]$, and $R_3 = [1500, 0.04]$.

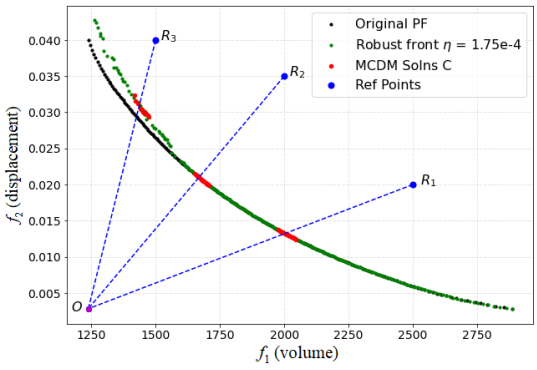


**Figure 5: Preferred robust solutions for the 4-bar truss problem using Scheme C.**

In MORODM Scheme A, 200 reference points are chosen to execute NSGA-III algorithm for 200 generations to arrive at PF

shown in black dots in Figure 4a. Next, MCDM is performed on PF by supplying the reference points $R_1$, $R_2$, and $R_3$ to the R-NSGA-III algorithm with population size per reference point $r_p$ = 20 and shrinkage factor $\mu$ = 0.05. R-NSGA-III algorithm is then executed for 200 generations for R-MOS by keeping other GA parameters the same as in the previous example. Figure 4a represents three different sets of MCDM solutions corresponding to each reference point, highlighted in red dots that lie on the PF. Next, these MCDM solutions are checked for their robustness using the constraint in definition (4). The solutions that satisfy the robustness definition are the preferred robust solutions. These solutions obtained on implementing MORODM Scheme A are highlighted in red dots in Figure 4b. From the figure, it can be concluded that the MCDM solutions on PF corresponding to reference point $R_3$ are not Type-II robust for the given robustness parameters. A few MCDM solutions corresponding to $R_2$ are robust, whereas all the MCDM solutions corresponding to $R_1$ are robust.

In MORODM Scheme B, the PF obtained are checked for their robustness using the robustness definition (4). The Pareto-optimal solutions that satisfy the Type-II robustness are highlighted in green dots to represent the RF in Figure 4c revealing the fact that only a part of PF is robust. Next, the MCDM task is performed at reference points $R_1$, $R_2$, and $R_3$ using R-NSGA-III on the RF. The preferred robust solutions obtained are highlighted in red dots in Figure 4c. Again, no robust solutions are found corresponding to the reference point $R_3$ for the given Type-II robustness and R-NSGA-III parameters. It is to be noted that MORODM Schemes A and

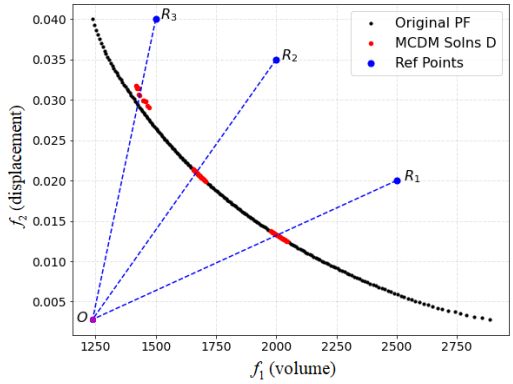


**Figure 6: Preferred robust solutions for the 4-bar truss problem using Scheme D.**

B provide the robust MCDM solutions that are present on the PF. Now, we implement the MORODM Scheme C that evaluates the RF and performs decision-making on the RF, instead of PF. Figure 5 represents the RF highlighted with green dots. Some parts of PF and RF coincide, whereas a few points on RF are shifted towards the dominated region of PF satisfying the Type-II robustness condition. Next, the MCDM task is performed using the R-MOS process from reference points $R_1$, $R_2$, and $R_3$ to arrive at preferred robust solutions highlighted in red dots in Figure 5. This scheme is able to find preferred robust solutions corresponding to reference point $R_3$, which were not possible to obtain by Schemes A and B. R-NSGA-III algorithm is executed for 1,000 generations by keeping other GA parameters the same as in the previous case. Note that this scheme requires finding the entire RF and then selecting the preferred robust solutions from RF.

Next, we implement MORODM Scheme D that implements R-NSGA-III algorithm to perform robust MCDM in a single step without computing the PF or RF. R-NSGA-III algorithm is executed for 1,000 generations by providing the reference points $R_1$, $R_2$, $R_3$, shrinkage factor $\mu$ = 0.05, and population size per reference point $r_p$ = 20 as input information for computing the preferred robust solutions. Solutions marked with red dots in Figure 6 are found. It can be seen in Figure 6 that preferred robust solutions corresponding to $R_1$ and $R_2$ lie on the PF, whereas that of $R_3$ is shifted inside the dominated region of PF. Interestingly, the entire RF was not required to be found by Scheme D.

From the two examples i.e. bi-objective test problem and the 4-bar truss problem discussed, we can conclude that the preferred robust solutions obtained by MOROMD Schemes A and B may not be possible to discover if they did not lie on the original PF. Although all preferred robust solutions may be possible to be obtained using MORODM Schemes C and D, due to the computational effectiveness, MORODM Scheme D is recommended and we demonstrate its further use on more problems involving three and more objectives.

## 4.3 Test Problem (3-objective)

This unconstrained MOO problem has three objectives and five design variables. Further details on this problem are presented in [8] as the first 3-objective test problem. For this problem, four reference points $R_1$ = [0.25, 0.25, 8.0], $R_2$ = [0.25, 1.0, 6.0], $R_3$ =[1.0, 0.25, 6.0], and $R_4$ = [1.0, 1.0, 1.5] are considered for the robust decision making task. The robustness parameters used in MORO are $\delta_i = \delta$, for $i$ = 1,2; and $\delta_i = 2\delta$ for $i$ >2. For this problem, the value of $\delta$, $H$, and $\eta$ is set to 0.01, 50, and 0.5, respectively.

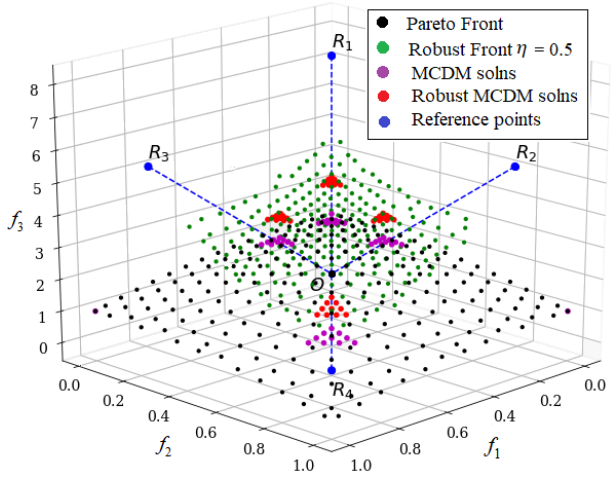


**Figure 7: 3-objective test problem results are shown. Green dots represent the RF. The magenta dots represent the preferred solutions on PF, whereas the red dots represent the preferred robust solutions obtained by Scheme D.**

Figure 7 represents the scatter plot of PF shown in black dots. The scatter plot of RF is highlighted in green dots. It can be seen that the points on RF are dominated by points on PF, confirming the fact that PO solutions are sensitive to variable uncertainties. RF solutions are dominated by PF solutions with respect to three objectives but are robust with respect to variable uncertainties. For the reference points $R_1$, $R_2$, $R_3$, and $R_4$, preferred PF solutions obtained using R-NSGA-III, executed with identical GA and robustness parameter values and run for 2,500 generations, are marked in magenta dots (lying on the PF). Note that these preferred solutions are not checked for robustness, but it is clear that these preferred PF (magenta) solutions do not lie on the RF.

Next, we implement Scheme D to perform the MORODM task for given reference points to find preferred robust solutions. The problem is solved for Type-II robustness and decision-making simultaneously using R-NSGA-III algorithm. The robust MCDM solutions obtained are highlighted in red dots, as shown in Figure 7. It is to be noted that these robust MCDM solutions (red dots) lie on the RF concluding that the MCDM solutions present on PF (in magenta color) are not Type-II robust with parameters values $\delta = 0.01$, $H = 50$, and $\eta = 0.5$.

MORODM Scheme D implemented on the three-objective test problem reveals the effectiveness of R-NSGA-III algorithm for performing robust decision-making. Since the MORODM solutions obtained here lie on the RF, it is clear that MORODM Schemes A and B will not provide any preferred robust solution for this problem. Again, Scheme C requires the computation of RF which is computationally expensive, hence, MORODM Scheme D is found to be the most effective among the other three MORODM Schemes for this problem.

## 4.4 River Pollution Problem (5-objective)

The river pollution problem is an unconstrained MaOP with five objectives and two design variables. Further details on this problem are discussed in [23]. A reference point $R = [-6.0, -3.4, 0.0, 10, 0.25]$ is used for the MORODM task. Robustness parameters $\delta = 0.02$, $H = 100$, and $\eta = 0.01$ are used for the Type-II robustness definition (4). The shrinkage factor $\mu$ and the population size per reference point ($r_p$) are set at 0.05 and 50, respectively, in R-NSGA-III.

A representative PF is computed using NSGA-III by using $p = 20$ to compute the reference directions using the Das-Dennis method [7] and the algorithm is executed for 50 generations with a tournament selection strategy. Other algorithmic parameters are kept the same as in the previous examples. Figure 8 shows the scatter plot of the PF and RF highlighted in orange and green dots, respectively. The RF is computed using the robustness definition of Type-II in NSGA-III. It is clear that RF front is a part of the original PF and comes from smaller values of $f_3$ and $f_4$ and larger values of $f_2$, but spread on $f_1$ stays more or less identical to that in the original PF. It is important to note that the computation of PF and RF is not needed for Scheme D, but we plot and show them here for the convenience of understanding and visualization of preferred robust solutions obtained using Scheme D, discussed below.

MORODM Scheme D is implemented on the river pollution problem. R-NSGA-III is executed for 100 generations by supplying the robustness parameters and R-NSGA-III parameters along with the

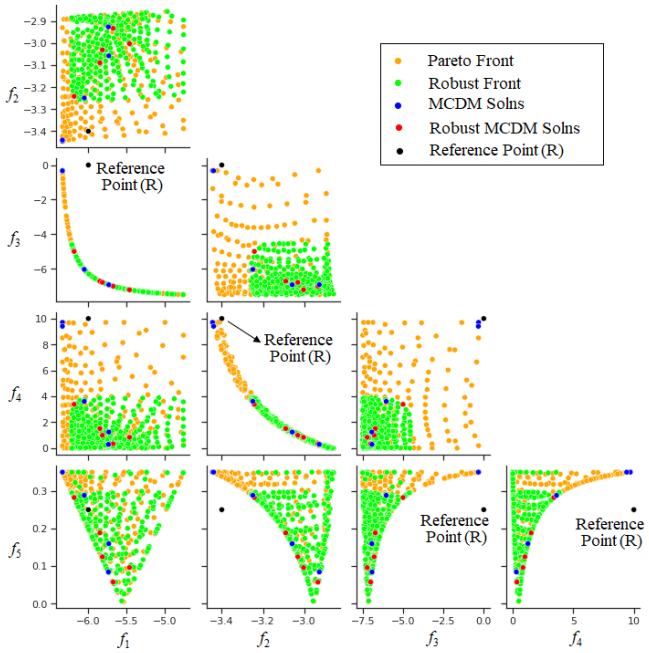


**Figure 8: Scatter plots for the river pollution problem are shown. Orange and blue dots represent PF and preferred solutions on PF, respectively. Black dots represent reference points. Green dots represent the RF, whereas the red dots represent the preferred robust solutions obtained by Scheme D.**

reference point as input information. The robust MCDM solutions obtained upon implementing MORODM Scheme D are highlighted in red dots in Figure 8. It can be seen from the figure that the MORODM solutions belong to the RF. However, a few of the MCDM solutions represented in blue markers are outside the RF revealing the need for robust MCDM. This example clearly shows how Scheme D can be applied to find a few preferred as well as robust solutions in a many-objective optimization problem.

## 4.5 Test Problem (8-objective)

The second three-objective test problem presented in [8] is extended to create an 8-objective test problem that has 10 design variables. A reference point $R$ = [1.0, 1.0, 1.0, 1.0, 1.0, 1.0, 1.0, 40.0] is used to perform MORODM Scheme D using R-NSGA-III. For performing the Type II robustness, the perturbation at different design variables are chosen as $\delta_i = \delta$, for $i$= 1,...,7; and $\delta_i = 2\delta$ for $i > 7$. The value $\delta = 0.075$, $H = 50$, and $\eta = 1.5$ is chosen for MaORO. The value of the shrinkage factor $\mu$ is set to 0.05 and the population size per reference point is set to 120.

MORODM Scheme D is implemented by executing R-NSGA-III algorithm for 2,000 generations and by keeping the other GA parameters the same as in the previous examples. Figure 9 represents the parallel coordinate plot (PCP) of the PF, RF, MCDM solutions, and MORODM solutions. The gray color lines represent the PF obtained using NSGA-III, the magenta color lines represent the MCDM solutions at PF, the green color lines represent Type-II RF obtained using NSGA-III, and the red color lines represent the

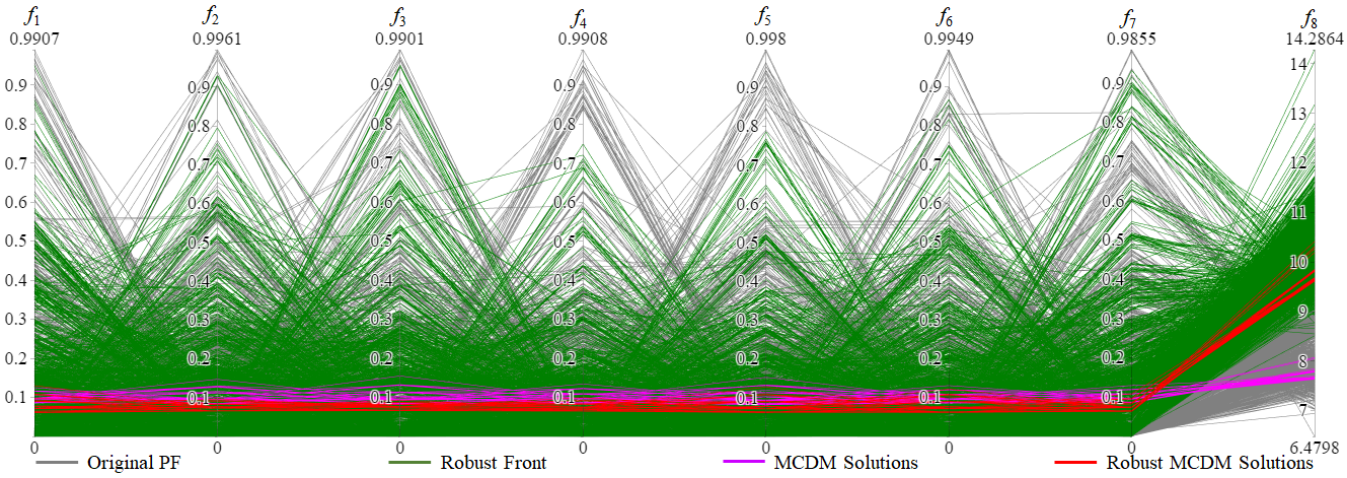


**Figure 9: Parallel coordinate plot (PCP) for the 8-objective problem is shown. Gray lines represent PF obtained using NSGA-III. Magenta lines represent the preferred (non-robust) solutions on PF. Green color lines represent the RF, whereas red color lines represent the preferred robust solutions obtained by Scheme D.**

robust MCDM solutions obtained using R-NSGA-III algorithm implemented in MORODM Scheme D. It is to be noted that MORODM Scheme D does not require PF or RF computation, here we plot it for the reference of highlighting the robust MCDM solutions.

From PCP in Figure 9, it can be inferred that the range of RF has shrunk in $f_1$-$f_7$ objectives. However, the objective $f_8$ is shifted towards relatively higher values as compared to $f_8$ objective values in the original PF. The preferred robust solutions obtained by implementing MORODM Scheme D highlighted in red lines belong to the RF. MORODM performed on the 8-objective test problem highlights the usefulness of R-NSGA-III in efficiently computing the preferred robust solution and performing a robust decision-making task.

From the test problems and real-world engineering problems discussed in this section, it can be concluded that MORODM Scheme D using R-NSGA-III algorithm is a computationally efficient procedure to perform the MORODM task to arrive at preferred robust solutions. The ability of R-NSGA-III to accommodate the Type-II robustness definition and perform decision-making tasks simultaneously without evaluating PF or RF independently makes it computationally efficient as compared to other MORODM schemes proposed here.

## 5 CONCLUSIONS

This paper has emphasized the concept of multi-objective robust optimization with decision-making (MORODM). Four different MORODM schemes have been proposed and implemented on three benchmark problems and two real-world engineering problems to find the preferred solution(s) on the robust front (RF), instead of the Pareto front (PF). Schemes A and B have evaluated PF followed by the robustness computation and decision-making preferences in a different order. The robust MCDM solutions obtained using these two schemes are robust solutions lying on the original PF. In some occasions, both schemes have resulted in generating no robust solution for certain reference points, indicating that this can be a possibility for certain MORODM approaches. Scheme C has addressed this limitation by first performing MORO to arrive at RF directly, instead of finding a PF and then choosing robust solutions from it, and then performing an MCDM task of choosing the preferred robust solution(s). However, Scheme C has a relatively higher computational cost due to the robustness definition check needed for every solution on the RF. Scheme D has addressed this limitation by including the robustness definition in the reference point-based MCDM procedure known as R-NSGA-III, so that the robustness definition has been applied to find preferred robust solutions. The results on problems have revealed that Scheme D makes an efficient MORODM task by performing robustness-check and decision-making simultaneously to save computational efforts for generating the preferred robust solutions.

In the future, other existing R-EMO algorithms such as R-NSGA-II [13], RD-NSGA-II [9], and MOEA/D [19, 31] among others can be used in the MORODM procedure and their computational effectiveness in performing robust MCDM can be evaluated. Also, the effect of robustness parameters $\delta$, $H$, $\eta$ and R-NSGA-III parameters $\mu$, $r_p$ on MORODM schemes can be studied further. Shrinkage factor ($\mu$) and population size per reference point ($r_p$) in NSGA-III are user-defined values that can be selected according to the maximum function evaluations calculated in terms of population size and the number of generations in GA, and convergence criteria. The robustness parameters are also user-defined values that can be appropriately selected according to the computational budget and permissible uncertainty level of the problem. Moreover, the effectiveness of R-NSGA-III algorithm for performing MORODM tasks can be tested on more challenging test problems proposed in [21]. The strategies such as the ones proposed in [2] and [32] can be implemented to improve the computational complexity of the EAs for performing the MORODM tasks to arrive at preferred robust solutions.

MORODM can also be applied to scalarization function-based MCDM techniques, such as NIMBUS and Pareto Race, for interactive and informed MORODM tasks using an effective visualization method [28, 29]. Also, the procedure for MORODM can be extended to handle constrained MOO and MaOP with uncertainty by introducing and quantifying the reliability parameter to arrive at robust and reliable preferred solutions [11]. Though this extension can be developed to perform multi-objective robust and reliable optimization and decision-making tasks, it should be noted that incorporating reliability as an additional constraint along with the robustness constraint can make the optimization task harder with increased computational complexity.

## REFERENCES


[1] J. Blank and K. Deb. 2020. pymoo: Multi-Objective Optimization in Python. *IEEE Access* 8 (2020), 89497–89509.

[2] Jürgen Branke. 2000. Efficient evolutionary algorithms for searching robust solutions. In *Evolutionary Design and Manufacture*. Springer, 275–285.

[3] John Telfer Buchanan. 1997. A naive approach for solving MCDM problems: The GUESS method. *Journal of the Operational Research Society* 48, 2 (1997), 202–206.

[4] Vira Chankong and Yacov Y Haimes. 2008. *Multiobjective decision making: theory and methodology*. Courier Dover Publications.

[5] FY Cheng and XS Li. 1999. Generalized center method for multiobjective engineering optimization. *Engineering Optimization* 31, 5 (1999), 641–661.

[6] Yuan Chi, Yan Xu, and Rui Zhang. 2020. Many-objective robust optimization for dynamic var planning to enhance voltage stability of a wind-energy power system. *IEEE Transactions on Power Delivery* 36, 1 (2020), 30–42.

[7] Indraneel Das and John E Dennis. 1998. Normal-boundary intersection: A new method for generating the Pareto surface in nonlinear multicriteria optimization problems. *SIAM journal on optimization* 8, 3 (1998), 631–657.

[8] Kalyanmoy Deb and Himanshu Gupta. 2005. Searching for robust Pareto-optimal solutions in multi-objective optimization. In *International conference on evolutionary multi-criterion optimization*. Springer, 150–164.

[9] Kalyanmoy Deb and Abhishek Kumar. 2007. Interactive evolutionary multi-objective optimization and decision-making using reference direction method. In *Proceedings of the 9th annual conference on Genetic and evolutionary computation*. 781–788.

[10] Kalyanmoy Deb and Abhay Kumar. 2007. Light beam search based multi-objective optimization using evolutionary algorithms. In *2007 IEEE Congress on Evolutionary Computation*. IEEE, 2125–2132.

[11] Kalyanmoy Deb, Dhanesh Padmanabhan, Sulabh Gupta, and Abhishek Kumar Mall. 2007. Reliability-based multi-objective optimization using evolutionary algorithms. In *Evolutionary Multi-Criterion Optimization: 4th International Conference, EMO 2007, Matsushima, Japan, March 5-8, 2007. Proceedings 4*. Springer, 66–80.

[12] Kalyanmoy Deb, Amrit Pratap, Sameer Agarwal, and TAMT Meyarivan. 2002. A fast and elitist multiobjective genetic algorithm: NSGA-II. *IEEE transactions on evolutionary computation* 6, 2 (2002), 182–197.

[13] Kalyanmoy Deb and J Sundar. 2006. Reference point based multi-objective optimization using evolutionary algorithms. In *Proceedings of the 8th annual conference on Genetic and evolutionary computation*. 635–642.

[14] Warren A Hall and Yacov Y Haimes. 1976. The surrogate worth trade-off method with multiple decision-makers. In *Multiple Criteria Decision Making Kyoto 1975*. Springer, 207–233.

[15] Fatemeh Jalalvand, Hasan Hüseyin Turan, Sondoss Elsawah, and Michael J Ryan. 2020. A multi-objective risk-averse workforce planning under uncertainty. In *2020 IEEE Symposium Series on Computational Intelligence (SSCI)*. IEEE, 1626–1633.

[16] Andrzej Jaszkiewicz and Roman Słowiński. 1999. The 'Light Beam Search' approach–an overview of methodology applications. *European Journal of Operational Research* 113, 2 (1999), 300–314.

[17] Pekka Korhonen and Jyrki Wallenius. 1988. A Pareto race. *Naval Research Logistics* 35, 6 (1988), 615–623.

[18] Pekka Korhonen and Guang Yuan Yu. 2000. Quadratic Pareto race. In *New Frontiers of Decision Making for the Information Technology Era*. World Scientific, 123–142.

[19] Ke Li, Renzhi Chen, Geyong Min, and Xin Yao. 2018. Integration of Preferences in Decomposition Multiobjective Optimization. *IEEE Transactions on Cybernetics* 48, 12 (2018), 3359–3370. https://doi.org/10.1109/TCYB.2018.2859363

[20] Kaisa Miettinen. 2012. *Nonlinear multiobjective optimization*. Vol. 12. Springer Science & Business Media.

[21] Seyedali Mirjalili and Andrew Lewis . 2015. Hindrances for robust multi-objective test problems. *Applied Soft Computing* 35 (2015), 333–348.

[22] Hirotaka Nakayama and Yoshikazu Sawaragi. 1984. Satisficing trade-off method for multiobjective programming. In *Interactive decision analysis*. Springer, 113–122.

[23] Subhash C Narula and HRoland Weistroffer. 1989. A flexible method for nonlinear multicriteria decision-making problems. *IEEE Transactions on Systems, Man, and Cybernetics* 19, 4 (1989), 883–887.

[24] Shokoufeh Pourshahabi, Gholamreza Rakhshandehroo, Nasser Talebbeydokhti, Mohammad Reza Nikoo, and Fariborz Masoumi. 2020. Handling uncertainty in optimal design of reservoir water quality monitoring systems. *Environmental Pollution* 266 (2020), 115–211.

[25] Yash Vesikar, Kalyanmoy Deb, and Julian Blank. 2018. Reference point based NSGA-III for preferred solutions. In *2018 IEEE symposium series on computational intelligence (SSCI)*. IEEE, 1587–1594.

[26] Andrzej P Wierzbicki. 1980. The use of reference objectives in multiobjective optimization. In *Multiple criteria decision making theory and application*. Springer, 468–486.

[27] Andrzej P Wierzbicki. 1999. Reference point approaches. In *Multicriteria decision making*. Springer, 237–275.

[28] Deepanshu Yadav, Deepak Nagar, Palaniappan Ramu, and Kalyanmoy Deb. 2023. Visualization-aided Multi-Criteria Decision-Making using Interpretable Self-Organizing Maps. *European Journal of Operational Research* (2023). https://doi.org/10.1016/j.ejor.2023.01.062

[29] Deepanshu Yadav, Palaniappan Ramu, and Kalyanmoy Deb. 2022. Visualization-aided Multi-criterion Decision-making Using Reference Direction Based Pareto Race. In *2022 IEEE Symposium Series on Computational Intelligence (SSCI)*. 125–132. https://doi.org/10.1109/SSCI51031.2022.10022083

[30] Abed Zabihian-Bisheh, Pooya Pourrezaie-Khaligh, Hamed Farrokhi-Asl, Stanley Frederick WT Lim, Masoud Rabbani, and Mohammad Khamechian. 2022. Multi-depot green capacitated location routing problem considering uncertainty and in-facility queuing. *Cleaner Waste Systems* 2 (2022), 100011.

[31] Qingfu Zhang and Hui Li. 2007. MOEA/D: A multiobjective evolutionary algorithm based on decomposition. *IEEE Transactions on evolutionary computation* 11, 6 (2007), 712–731.

[32] Qi Zhou, Ping Jiang, Xiang Huang, Feng Zhang, and Taotao Zhou. 2018. A multi-objective robust optimization approach based on Gaussian process model. *Structural and Multidisciplinary Optimization* 57, 1 (2018), 213–233.